Preparation of Poly(lactic acid) Fiber by Dry-Jet-Wet-Spinning. I. Influence of Draw Ratio on Fiber Properties

Bhuvanesh Gupta,[1] Nilesh Revagade,[1] Nishat Anjum,[1] Björn Atthoff,[2] Jöns Hilborn[2]

[1]*Department of Textile Technology, Indian Institute of Technology, New Delhi, India*
[2]*Polymer Chemistry Programme, Ångström Laboratory, Uppsala University, Sweden*

Received 18 March 2005; accepted 1 August 2005
DOI 10.1002/app.23497
Published online in Wiley InterScience (www.interscience.wiley.com).

ABSTRACT: Poly(lactic acid) fiber was prepared by dry-jet-wet spinning of the polymer from chloroform solution and with methanol as the precipitating medium. The as-spun fiber was subsequently made into high strength fiber by two-step process of drawing at a temperature of 90°C and subsequent heat setting in the temperature range of 120°C. The draw ratio had significant influence on the crystallinity and the tensile strength of the fiber. The fiber with the tenacity of 0.6 GPa and modulus of 8.2 GPa was achieved at a draw ratio of 8. The differential scanning calorimetry revealed an increase in the glass-transition temperature with the increase in the draw ratio, which suggests the orientation of chains during the drawing process. The surface morphology of the filament as revealed by scanning electron microscopy shows that fibers are porous in nature, but a significant reduction in the porosity and pore size of the fiber was observed with the increase in the draw ratio. © 2006 Wiley Periodicals, Inc. J Appl Polym Sci 100: 1239–1246, 2006

Key words: poly(lactic acid); dry-jet-wet spinning; biodegradable fiber

INTRODUCTION

Polylactic acid (PLA) represents one of the most promising biodegradable polymers because of its wide acceptability in a number of medical domains, such as drug delivery systems,[1,2] sutures,[3–5] porous meshes or foams, or composites.[6–12] The favorable degradation behavior associated with the optimum mechanical characteristics and the biocompatibility of this polymer has led to considerable investigations on the development of the material for medical applications. The interesting aspect of the polymer is that the material undergoes hydrolysis of the ester linkage in the main chain during *in vivo* condition and leads to the formation of nontoxic lactic acid, which is subsequently consumed in the carbohydrate metabolism in the human body.

Among the PLA-based medical devices, the fibrous materials have generated considerable momentum in tissue engineering.[13–16] This unique way of organ reconstruction offers several advantages over the conventional transplantation method as the transplant rejection is overcome and there is no donor requirement as cells belong to the patient himself. Several studies have been carried out to prepare fibers that have better tensile strength so that the fiber retains mechanical stability initially for sufficient time during the functional use.[17–19] Different spinning methods have been used by different workers for the preparation of the PLA fiber, which include the melt spinning[17,20–26] and dry spinning.[21,22,27–29] The spun fibers are subsequently subjected to drawing and heat setting to achieve the material with high tensile strength. In these studies, the development of the fiber with high mechanical strength has been the prominent aspect. The melt spinning of the PLA has been an appropriate approach since a long time where Schneider developed the fiber with tensile stress of 0.5–0.7 GPa.[20] Subsequently, Eling et al.[21] carried out melt spinning and subsequent drawing to produce fibers with tensile strength of 0.5 GPa and modulus of 7 GPa. The studies of Penning et al.[22] on spinning at a higher temperature of 210°C instead of usual 185°C and further drawing process produced fiber with tensile strength of 0.53 GPa, but the modulus enhanced to 9 GPa. The recent work by Fambri et al.[23] on hot drawing of the spun fibers led to fibers with impressive strength of 0.87 GPa and modulus of 9.2 GPa, which are much higher values than those observed by Yuan et al.[24] for the hot drawn samples (3.6–5.4 GPa). Cicero and Dorgan[17] reported the PLA fiber of maximum tensile strength and modulus of 0.38 and 3.2 GPa, respectively, produced by continuous two-step melt-spinning process. The high-speed melt spinning (5000 m/min) and spin drawing process was used by Schmack et al.[25] to produce mechanically strong fiber; however, the maximum strength and modulus re-

Correspondence to: B. Gupta (bgupta@textile.iitd.ernet.in).

mained limited to 0.46 and 6.3 GPa, respectively. Similar strength has been observed in the high-speed melt spinning of the PLA by Mezghani and Spruiell.[26] It is important to mention here that severe thermal degradation takes place during the melt spinning of the polymer (~70% loss), which limits the mechanical strength of the resultant fiber.[20]

The wet spinning and the dry spinning have been effective in controlling the degradation due to relatively lower processing temperatures, thereby providing better tensile properties of the fiber. The research group of Pennings and coworkers[27,28] has observed that the dry spinning provides high strength fiber (1.5 GPa) at high spinning rates of greater than 180 m/min. The group has reported a high tenacity of 2.1 GPa and a modulus of 16 GPa by dry spinning and hot drawing of PLA from solutions in chloroform and toluene, which no other study was ever able to report.[27] It is known that the drawing conditions affect the molecular orientation and crystallization process, which in turn is reflected in the tensile characteristics of the fiber. The hot drawing in two different temperature regions, i.e., up to 180°C in which deformation takes place in the semicrystalline state and between 180 and 190°C where deformation is in the liquid state has been observed to produce fiber with very high tensile strength of 2.3 GPa.[29] This is a much higher value than the one (0.53 GPa) usually observed in the melt spinning of PLA.[22]

We have been working on the development of textile scaffolds for the human urinary bladder reconstruction. In this context, we have developed bioreceptive poly(ethylene terephthalate) (PET) knittings and films where urothelial cells and smooth muscle cells were seeded for their subsequent growth into a tissue.[30–33] Our approach is to move from biostable PET to biodegradable polyesters such as poly(lactic acid) (PLA) for scaffold development. The present work aims at developing PLA fiber, which has good strength and may be transformed into knitted scaffolds for human urinary bladder reconstruction. This is where our efforts are to develop the fiber on top of which we may immobilize collagen protein for subsequent growth of urothelial and smooth muscle cells.

Our attempt is to produce the PLA fiber by using a process where the polymer degradation is reduced to minimum. Attempts have been made to reduce the PLA degradation during spinning by adding additives like tri(nonylphenyl) phosphite prior to the processing.[34] It was observed that PLA degradation can be completely eliminated without adversely affecting the properties of PLA. But the addition of additives is always a least attractive technique when the intended applications are in the biomedical field. Looking at the different aspects of the fiber spinning by melt and solution spinning reported by different workers, we have undertaken this investigation on spinning of PLA by dry-jet-wet spinning. From the literature, it was observed that no detail study has been carried out in case of PLA fibers spun by dry-jet-wet spinning technique. Hence, the efforts were made to study the structure and mechanical properties of these fibers with variation of draw ratio. (Draw ratio is a well-defined physical quantity and is a direct measure of the amount of elongational deformation the material is undergoing.)

EXPERIMENTAL

Materials

Poly(lactic acid) (PLA) was received from Polymer laboratory, University of Uppsala, Sweden and was stored under vacuum at ambient conditions. Chloroform and methanol were supplied from Merck India. Chloroform was dried over P_2O_5 prior to the polymer dissolution. The viscosity of PLA was measured in chloroform using Ubbelhode viscometer in a constant temperature bath. The intrinsic viscosity was determined and the viscosity average molecular weight was calculated from the following equation.

$$\eta = KM_v^{\alpha}$$

where η is the intrinsic viscosity, M_v is the viscosity average molecular weight, K and α are the constants with values as 5.45×10^{-4} and 0.73, respectively.[35]

Spinning

PLA was dried at 110°C under vacuum for 24 h prior to the spinning. The polymer was dissolved in chloroform using a moisture-free glass assembly, under constant stirring at ambient conditions for 24 h. The polymer solution was subsequently spun on a spinning machine fabricated by Bradford University Research limited (Fig. 1).

The polymer solution was extruded through the spinneret of 0.5 mm into the coagulation bath containing methanol. Both the coagulation bath had methanol as the coagulant and collected using two sets of take-up rollers, both operating at the speed of 10 m/min. The air gap between the spinneret and coagulation bath was kept as 25 mm. The throughput rate was 0.4 g/min. The fiber was collected on bobbins and was subjected to drawing process in the second step.

Drawing

The as-spun fiber was subjected to drawing and heat-setting operations. The fiber was drawn to different draw ratios in the range of 2–10 at the drawing temperature of 90°C, followed by the heat setting at 120°C under taut conditions.

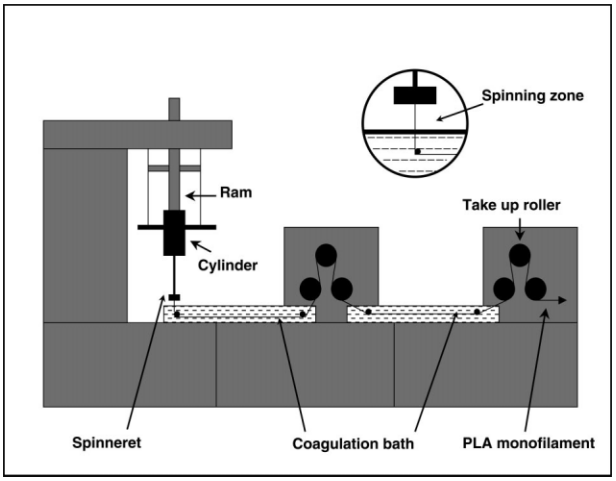

Figure 1 Schematic diagram of dry-jet-wet spinning of PLA fiber.

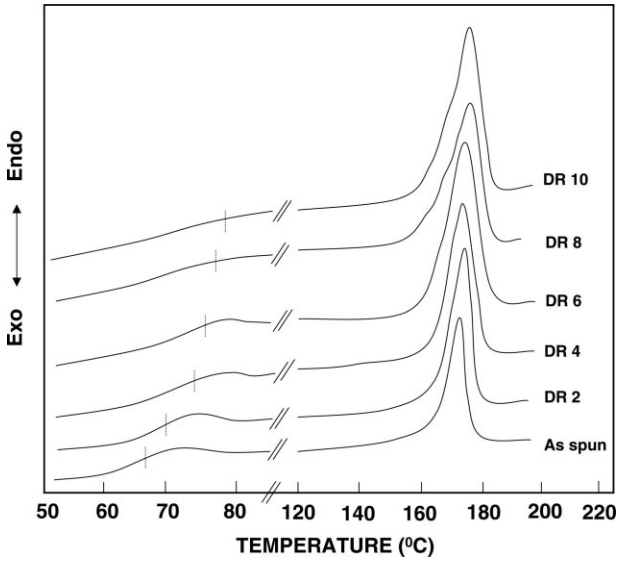

Figure 2 DSC thermograms of the PLA fibers drawn at different draw ratios (DR). Drawing temperature, 90°C; heat-setting temperature, 120°C.

X-ray diffraction

X-ray diffraction (XRD) patterns of the PLA filaments were recorded in the 2θ range of 10°–35° on a Phillips X-ray diffractometer equipped with a scintillation counter. CuKα radiation (wavelength, 1.54 A°) was used for X-ray diffraction experiments. The amorphous PLA sample was prepared by quenching of the molten polymer in liquid nitrogen.

The average lateral crystalline thickness was estimated from the broadening observed in the WAXD pattern recorded for 2θ range of 10°–35°, at a scanning rate of 2°/min. The integral breadth of the diffraction intensity arising from the imperfection of crystallites is measured in terms of $\beta_{1/2}$ (hkl). Higher the value of $\beta_{1/2}$ (hkl), the lower is the crystalline perfection.

Apparent crystal size was determined according to the Scherer's equation:

$$D(hkl) = \frac{K\lambda}{\beta \cos\theta}$$

where, β is the half width of the diffraction peak in radians, K is taken to be the unity, θ is the Bragg's angle, and λ is the wave length of the X-rays. The values of D (hkl) for (110) and (040) reflections were calculated.

TABLE I
Effect of Spinning Processing Conditions on Molecular Weight of PLA

Material	Intrinsic viscosity (dL/g)	Molecular weight (M_v) (10^5)	Drop in M_v (%)
PLA-dried chips	3.32	1.53	—
PLA as spun	3.19	1.45	5.20
PLA drawn	3.11g	1.39	9.15

Differential scanning calorimetry (DSC)

DSC studies on fibers were carried out on Perkin–Elmer DSC-7 system. Vacuum-dried samples were loaded and the thermograms were run in the temperature range of 40–200°C under nitrogen atmosphere at a heating rate of 10°C/min. The heat of fusion (ΔH_f) values were obtained from the area under the melting thermograms. The crystallinity was obtained by the following expression:

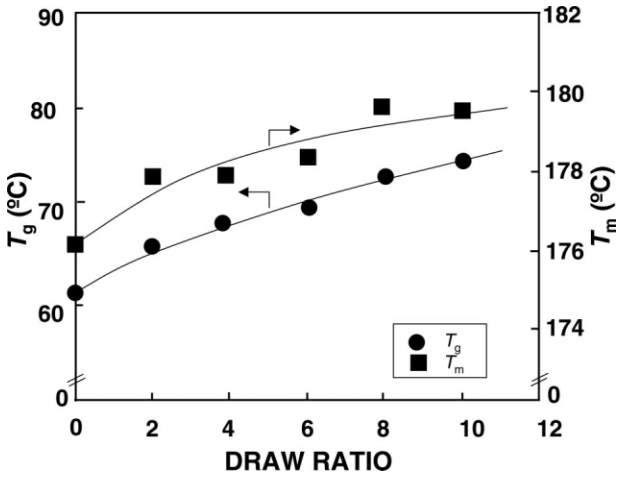

Figure 3 Variation of glass-transition temperature and melting temperature with the draw ratio of PLA fiber. Experimental conditions as in Figure 2.

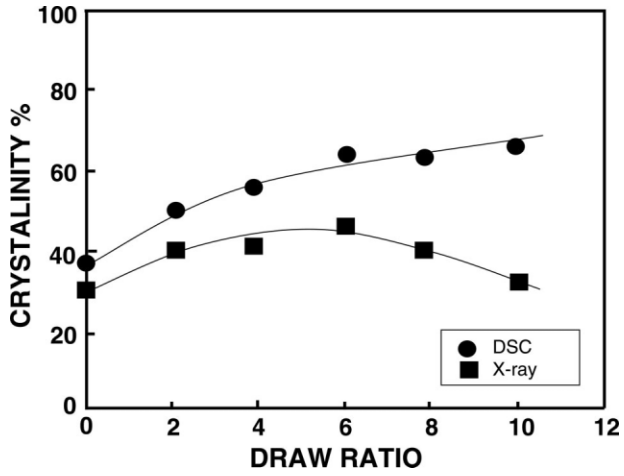

Figure 4 Variation of percent crystallinity with the draw ratio as measured from DSC and X-ray diffraction. Experimental conditions as in Figure 2.

$$\text{Crystallinity (\%)} = \frac{\Delta H_f}{\Delta H_{f(crys)}} \times \overline{100}$$

where, ΔH_f is the heat of fusion of the sample and $\Delta H_{f(crys)}$ is the heat of fusion of 100% crystalline PLA and was taken as 93.7 J/g.[36]

Mechanical properties

The tensile properties of PLA fibers were measured using an Instron tensile tester. All the experiments were carried out using gauge length of 50 mm and rate of testing as 50 mm/min.

Sonic modulus

Sonic modulus of fibers was measured on a pulse propagation meter (PPM 5R). The single filament was mounted between two transducers containing a piezoelectric ceramic crystal with a natural frequency of 5 kHz. The velocity of the longitudinal wave in the material was measured by having the fiber between two transducers. The sound velocity was measured by taking length and time measurement from the recorder as per the following equation.

$$C = \frac{\Delta l}{\Delta t}$$

Δl is the distance in mm, Δt is the transit time in μs, C is the velocity of sound in km/s. The Young's modulus was determined as per the equation.

$$E = \rho C^2$$

where ρ is the density (g/cc^3).

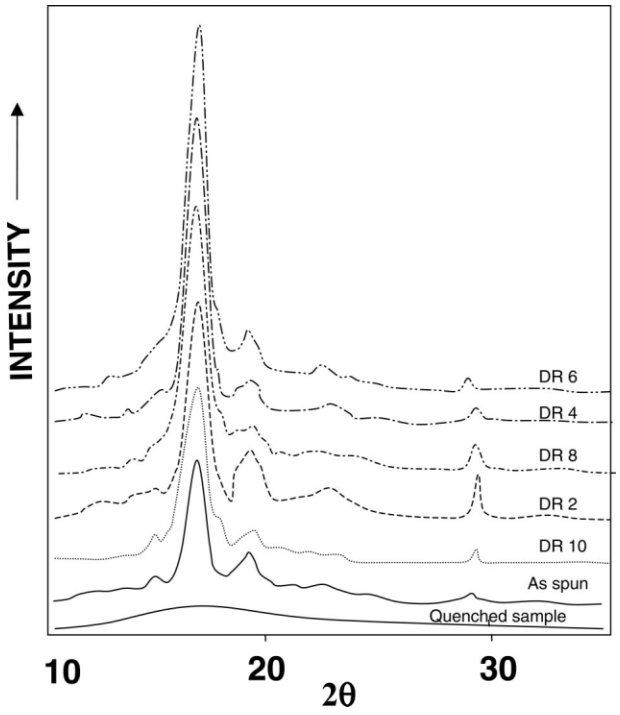

Figure 5 X-ray diffraction pattern of PLA fibers prepared at different draw ratios. Experimental conditions as in Figure 2.

The modulus in gram per denier (gpd) would therefore be obtained by the following equation.

$$E(gpd) = (E/\rho) = C^2K$$

where K is the conversion factor of 11.3.

Scanning electron microscope

The surface characteristics of fibers were studied using STEREOSCAN 360 (Cambridge Scientific Industries

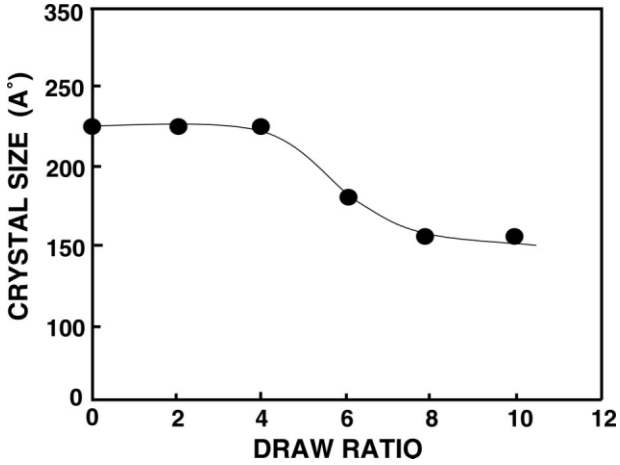

Figure 6 Crystal size variation with draw ratio.

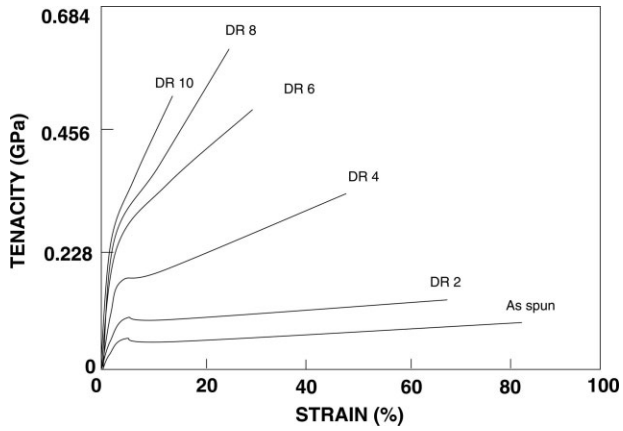

Figure 7 Stress–strain plots of the PLA fibers drawn at different draw ratios. Experimental conditions as in Figure 2.

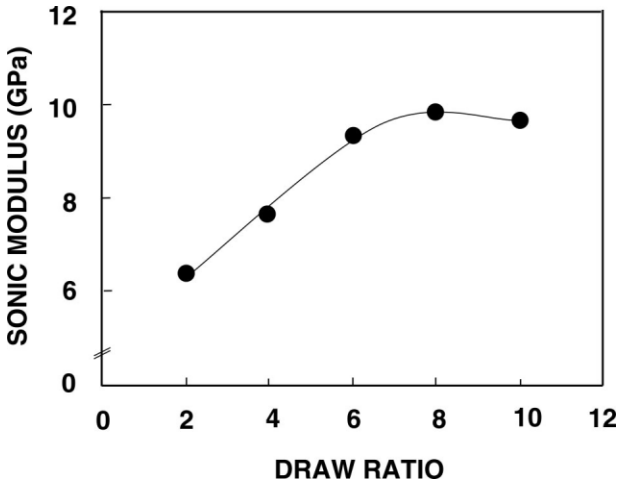

Figure 9 Variation of sonic modulus with the draw ratio in PLA fibers. Experimental conditions as in Figure 2.

Ltd.), scanning electron microscope, after coating them with silver.

RESULTS AND DISCUSSION

The polylactic acid (PLA) fibers were prepared by dry-jet-wet spinning method. The as-spun PLA fibers obtained by the dry-jet-wet spinning were subjected to the drawing and heat-setting operations. The intrinsic viscosity decreases from 3.32 dL/g to 3.19 dL/g after the spinning of this polymer from chloroform solution using methanol as the nonsolvent bath. The subsequent drawing of the filaments leads to further decrease in viscosity up to 3.11 dL/g giving an overall rather small decrease of 9.15% in viscosity average molecular weight (Table I). As-spun filament acquires some degree of molecular orientation due to the air gap provided in dry-jet-wet-spinning process.

The drawing of the fiber was carried out at a temperature range of 90°C, followed by the heat setting at 120°C. It is observed that both the draw ratio (DR) and heat-setting temperature play crucial role in establishing the crystalline structure and the morphology of the fiber. It is important to mention that under our spinning conditions, a maximum draw ratio of 10 could be achieved. This draw ratio is comparatively higher than that reported for is usually achieved in melt spinning of PLA. This may be due to the fact that the chain entanglement is largely suppressed in the solution state as compared with the polymer melt. Since the entanglements are the key factors in limiting the maximum drawability of a polymer, the low entanglements are effectively transferred to the fiber structure.[37]

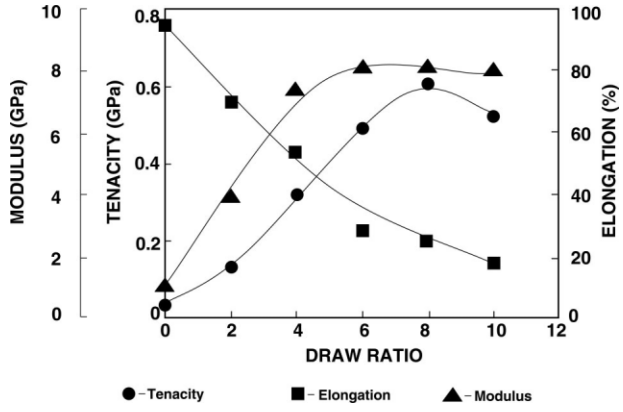

Figure 8 Variation of tenacity, modulus, and elongation with the draw ratio in PLA fibers. Experimental conditions as in Figure 2.

The DSC scans of fibers obtained at different draw ratios are shown in Figure 2. The as-spun fiber shows distinct presence of glass-transition temperature and the melting endotherm. The melting thermogram, however, became more pronounced and broader as the draw ratio is increased. The peak melting temperature also increases with the increase in the draw ratio (Fig. 3). The glass-transition temperature, T_g of the as-spun fiber was 61°C, which shows further increase to 76°C with the increase in the draw ratios. Our observations are different than the trend reported by Cicero et al.[18] for DSC studies on PLA fibers. The T_g did not show linear increase with draw ratio. Moreover, maximum T_g was around 65°C as compared with 76°C from our investigations.

As the glass transition is associated with the mobility in the amorphous region of the fiber, orientation is introduced in these regions during the drawing process. Further, the crystalline regions in a semicrystalline polymer are known to act as the anchors between the amorphous regions and therefore tend to restrict the molecular molbility.[38] The observed behavior of the T_g enhancement with drawing and heat setting may, therefore, be attributed to the cumulative effect

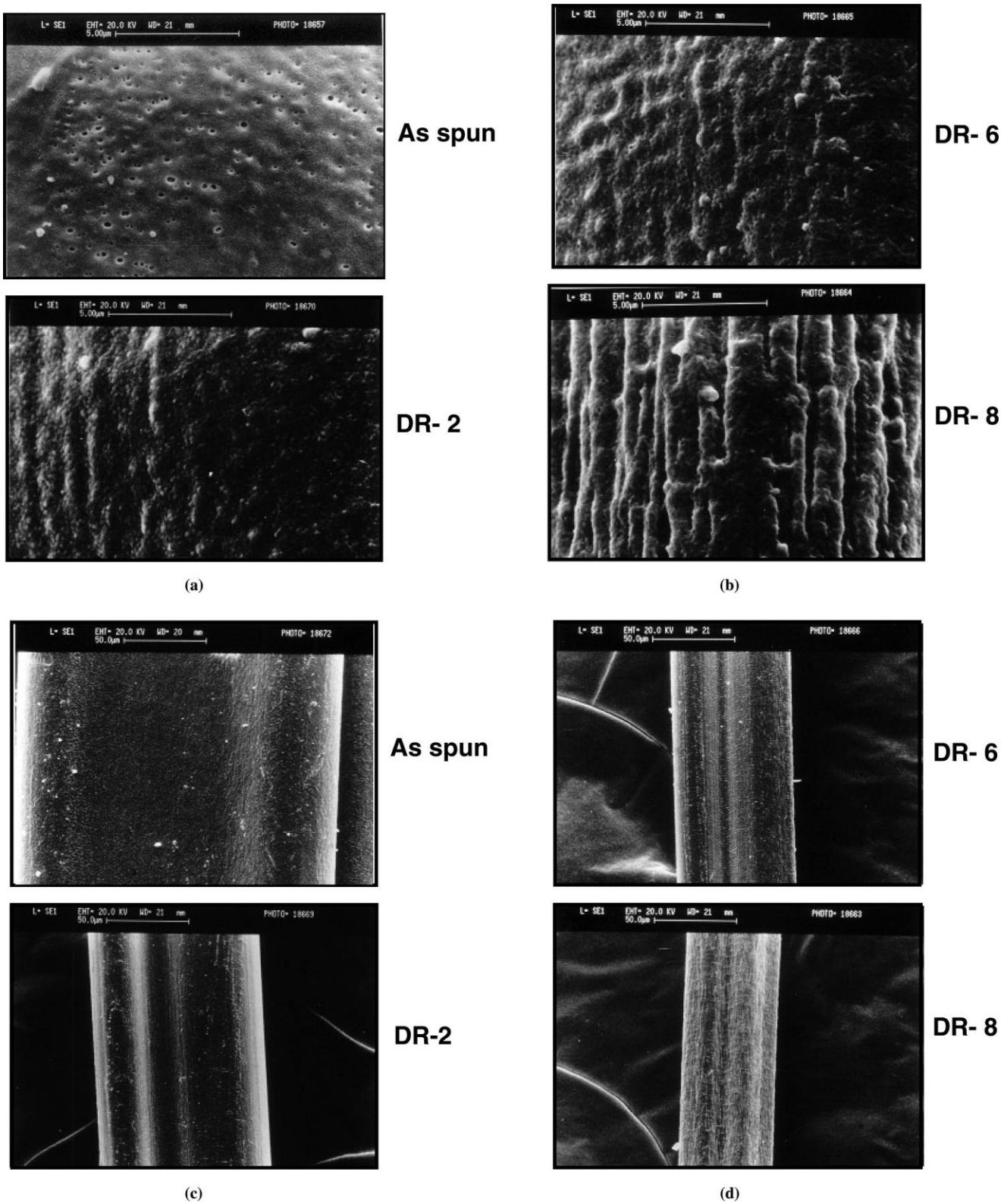

Figure 10 SEM of fibers drawn at different draw ratio. Experimental conditions as in Figure 2. (a) and (b) SEM of fibers at higher magnification; (c) and (d) SEM of fibers at lower magnification.

of the enhanced orientation in the amorphous region and the high crystallinity.[19] This reflects the impact of crystallinty originating during these steps on the diminishing mobility of polymer chains and has been observed by Fu et al.[37] for the poly(glycolide-*co*-lactide) fiber.

The investigations of Yuan et al.[24] have observed that DSC heating curve of as-spun sample is typical of a reflecting glass transition, crystallization, and melting. In our study, the as-spun filament was observed to be highly amorphous in nature (16–23% crystallinity) and therefore, the chains crystallize during heating in DSC. The results in Figure 2 are the outcome of the progressive hot drawing where the chains become highly oriented along the drawing direction and the fiber develops high crystallinity. The variation of the crystallinity as a function of the draw ratio, obtained from the heat of fusion in DSC thermograms, is presented in Figure 4. Undrawn samples and samples with lower draw ratio tend to crystalline during heating in DSC. The X-ray diffraction pattern of the fibers is presented in Figure 5. All diffractions lie at identical angles, and no additional diffraction peaks were visible in the drawn fibers, indicating that the crystalline phase dose not change during drawing process. The variation of crystal size with draw ratio is plotted in Figure 5. The crystal size decreases from 223 A° for as-spun fiber to 149 A° for a draw ratio of 10, indicating the crystal thinning during the drawing process.

The X-ray crystallinity increases up to DR 6, but then tends to decrease for further increases in the DR upto 10. It seems that the orientation-induced crystallization proceeds smoothly upto a draw ratio of 6 above which the fibrils are deformed and decrease in crystal size takes place (Fig. 6), which is reflected in the slight decrease in crystallinity. The trend in DSC is different than the one observed by X-ray diffraction as the chains undergo crystallization during the heating process and add to the overall crystallinity. The enhancement in the melting temperature of the fiber from 177°C for as-spun to 180°C with increasing draw ratio upto 8 is supportive of the perfection of crystalline zone with the draw ratio (Fig. 3). At draw ratio of 10, overdrawing is observed with whitening of the sample associated with void generation. This may also lead to decrease in crystallinity as observed by X-ray diffraction.

The tensile behavior of filaments at different draw ratios is presented in Figure 7. The as-spun fiber shows the maximum elongation and a low level of strength. The yield point in the fiber is well defined and is evident as a very long necking period where the molecular chains uncoil and are oriented to take up higher stresses subsequently. This may be well understood from the highly amorphous and nonoriented nature of the as-spun fiber. With increasing draw ratio, the stress–strain curves shift, which are consistent with increasing orientation and crystallinity. The maximum strength is shown at a draw ratio of 8. At draw ratio of 10, the decrease in strength can be associated with void generation due to overdrawing.

The variation of tenacity, modulus, and elongation of the fiber with the draw ratio is presented in Figure 8. The modulus of the fiber also shows a sharp enhancement with the increase in the draw ratio. A maximum tenacity of 0.6 GPa and modulus of 8.2 GPa were achieved for a draw ratio of 8. The elongation on the other hand shows continuous decrease with the increase in the draw ratio, as evident from 71% for as-spun to 16% for a draw ratio of 10. The significantly high strength of the fiber thus produced is the outcome of the high orientation of molecular chains and crystallinity. The sonic modulus of the fibers is indicative of the orientation that originates at different draw ratios (Fig. 9). Schmack et al.[36] observed similar influence of the draw ratio on orientation and crystallnity.

The SEM of fibers is presented in Figures 10(a)–10(d). The as spun fiber shows a porous structure throughout the surface. The pore size in as-spun fiber ranges between 5 and 10 μm. The drawing of the fiber at 90°C and subsequent heat setting at 120°C leads to gradual change in the surface morphology. Although, the drawing leads to collapse of the porous structure, the surface is still porous at higher draw ratios. The porosity becomes very little and the pore size also decreases to $\sim$2 μm at a draw ration of 10.

CONCLUSIONS

The dry-jet-wet spinning of polylactic acid produces the fiber where the molecular weight degradation during the spinning is very small and a significant advantage is achieved as compared with the melt-spinning process. The fiber acquires some orientation even before the coagulation process, which helps in further consolidating the fiber strength. The maximum draw ratio of 10 was achieved for the fiber. The draw ratio plays an important role in the structural development of the fiber. The orientation and crystallinity increase with the increase in the draw ratio. The tensile strength of the fiber also increases for an increase in the draw ratio upto 8 and then tends to decrease. The drawing leads to collapse of the porous structure; the surface is porous still at higher draw ratio. The porosity becomes negligible and pores get stretched during the process.

References

1. Kenawy, El.-R.; Bowlin, G. L.; Mansfield, K.; Layman, J.; Simpson, D. G.; Sanders, E. H.; Wnek, G. E. J Contr Rel 2002, 81, 57.
2. Grandfils, C.; Flandroy, P.; Jèrôme, R. J Contr Rel 1996, 38, 109.
3. Horton, C. E.; Adamson, J. E.; Mladick, R. A.; Carraway, J. H. Am Surg 1974, 729.
4. Reed, A. M.; Gilding, D. K. Polymer 1981, 22, 494.
5. Seal, B. L.; Otero, T. C.; Panitch, A. Mater Sci Eng R 2001, 34, 147.
6. Shi, G. X.; Cai, Q.; Wang, C. Y.; Lu, N.; Wang, S. G.; Bei, J. Z. Polym Adv Technol 2002, 13, 227.
7. Ma, P. X.; Zhang, R. Y. J Biomed Mater Res 1999, 46, 60.

8. Lu, L.; Peter, S. J.; Lyman, M. D.; Lai, H. L.; Leite, S. M.; Tamada, J. A.; Vacanti, J. P.; Langer, R.; Mikos, A. G. Biomaterials 2000, 21, 1595.
9. Mikos, A. G.; Thorsen, A. J.; Czerwonka, L. A.; Bao, Y.; Langer, R.; Winslow, D. N.; Vacanti, J. P. Polymer 1994, 35, 1068.
10. Kasuga, T.; Ota, Y.; Nogami, M.; Abe, Y. Biomaterials 2001, 22, 19.
11. Gogolewski, S.; Pineda, L.; Busing, C. M. Biomaterials 2000, 21, 2513.
12. Chu, C. R.; Coutts, R. D.; Yoshioka, M.; Harwood, F. L.; Monosov, A. Z.; Amiel, D. J Biomed Mater Res 1995, 29, 1147.
13. Dattilo, P. P., Jr.; King, M. W.; Cassill, N. L.; Leung, J. C. J Text App Technol Manag 2002, 2, 1.
14. Widmer, M. S.; Gupta, P. K.; Lu, L.; Meszlenyi, R. K.; Evans, G. R. D.; Brandt, K.; Savel, T.; Gurlek, A.; Patrick, C. W., Jr.; Mikos, A. G. Biomaterials 1945, 1998, 19.
15. Steuer, H.; Fadele, R.; Müller, E.; Müller, H.-W.; Planck, H.; Schlosshauer, B. Neurosci Lett 1999, 165, 277.
16. Kim, K.; Yu, M.; Zong, X.; Chiu, J.; Fang, D.; Seo, Y.; Hsiao, B. S.; Chu, B.; Hadjiargyrou, M. Biomaterials 2003, 24, 4977.
17. Cicero, J. A.; Dorgan, J. R. J Polym Envir 2002, 9, 1.
18. Cicero, J. A.; Dorgan, J. R.; Janzen, J.; Garrett, J.; Runt, J.; Lin, J. S. J Appl Polym Sci 2002, 86, 2828.
19. Cicero, J. A.; Dorgan, J. R.; Garrett, J.; Runt, J.; Lin, J. S. J Appl Polym Sci 2002, 86, 2839.
20. Schneider, A. K. U.S. Pat. 3,636,956 (1972).
21. Eling, B.; Gogolewski, A.; Pennings, A. J. Polymer 1982, 23, 1587.
22. Penning, J. P.; Dijkstra, H.; Pennings, A. J. Polymer 1993, 34, 942.
23. Fambri, L.; Pegoretti, A.; Fenner, R.; Incardona, S. D.; Migliaresi, C. Polymer 1997, 38, 79.
24. Yuan, X.; Mak, A. F. T.; Kwok, K. W.; Yung, B. K. O.; Yao, K. J Appl Polym Sci 2001, 81, 251.
25. Schmack, G.; Tandler, B.; Vogel, R.; Beyreuther, R.; Jacobsen, S.; Fritz, H. G. J Appl Polym Sci 1999, 73, 2785.
26. Mezghani, K.; Spruiell, J. E. J Polym Sci Polym Phys 1998, 36, 1005.
27. Leenslag, J. W.; Pennings, A. J. Polymer 1987, 28, 1695.
28. Postema, A. R.; Luiten, A. H.; Oostra, H.; Pennings, A. J. J Appl Polym Sci 1990, 39, 1275.
29. Postema, A. R.; Pennings, A. J. J Appl Polym Sci 1989, 37, 2351.
30. Gupta, B.; Hilborn, J.; Hollenstein, C.; Plummer, C. J. C.; Xandropolous, N.; Houriet, R. J Appl Polym Sci 2000, 78, 1083.
31. Gupta, B.; Hilborn, J.; Bisson, I.; Frey, P.; Plummer, C. J Appl Polym Sci 2001, 81, 2993.
32. Gupta, B.; Plummer, C.; Hilborn, J.; Bisson, I.; Frey, P. Biomaterials 2002, 23, 863.
33. Bisson, I.; Kosinski, M.; Ruault, S.; Gupta, B.; Hilborn, J.; Florian, W.; Frey, P. Biomaterials 2002, 23, 3149.
34. Cicero, J. A.; Dorgan, J. R.; Dec, S. F.; Knauss, D. M. Poly Deg Stab 2002, 78, 95.
35. Smith, P.; Lemstra, P. J.; Booij, H. C. J Polym Sci Polym Phys Ed 1981, 19, 877.
36. Schmack, G.; Jehnichen, D.; Vogel, R.; Tändler, B.; Beyreuther, R.; Jacobsen, S.; Fritz, H. -G. J Biotech 2001, 86, 151.
37. Fu, B. X.; Hsiao, B. S.; Chen, G.; Zhou, J.; Koyfman, I.; Jamiolkowski, D. D.; Dormier, E. Polymer 2002, 43, 5527.
38. Jamshidi, K.; Hyon, S.-H.; Ikada, Y. Polymer 1988, 29, 2229.